Published in final edited form as:
Biomacromolecules. 2005 ; 6(6): 2961–2968.

Oligonucleotide structure influences the interactions between cationic polymers and oligonucleotides

Sumati Sundaram[1], **Sandra Viriyayuthakorn**[2], and **Charles M. Roth**[1,2,*]

1*Department of Chemical & Biochemical Engineering, 98 Brett Road, Piscataway, NJ 08854, USA*

2*Department of Biomedical Engineering, Rutgers University, 98 Brett Road, Piscataway, NJ 08854, USA*

Abstract

We examined the effect of oligodeoxynucleotide (ODN) structure on the interactions between cationic polymers and ODNs. Unstructured and hairpin structured ODNs were used to form complexes with the model cationic polymer, poly-L-lysine (pLL), and the characteristics of these polymer-ODN interactions were subsequently examined. We found that hairpin structured ODNs formed complexes with pLL at slightly lower pLL:ODN charge ratios as compared to unstructured ODNs and that, at high charge ratios, greater fractions of the hairpin ODNs were complexed, as measured by dye exclusion. The dissociation of pLL-ODN interactions was tested further by challenge with heparin, which induced complex disruption. Both the kinetics and heparin dose response of ODN release were determined. The absolute amount and the kinetic rate of ODN release from the complexes of pLL and unstructured ODN were greater, as compared to hairpin ODNs. Our results therefore highlight the role of ODN structure on the association-dissociation behavior of polymer-ODN complexes. These findings have implications for the selection of ODN sequences and design of polymeric carriers used for cellular delivery of ODNs.

Introduction

Antisense technology employs short, single-stranded oligodeoxynucleotides (ODNs), typically 12-25 bases long, to inhibit gene expression by binding to complementary mRNA via Watson-Crick base pairing. Over the last decade, antisense approaches have been developed for therapeutic purposes as well as for biotechnological applications[1]. However, the widespread use of antisense ODNs is still hindered by several obstacles. Prominent among them is the ineffective cellular delivery of ODNs, which remains a major hurdle in the utilization of ODN-based technologies[2].

Numerous polymeric delivery agents have been developed to enhance cellular uptake while also protecting the ODNs from degradation[3,4,5]. Progress in vector development for ODN delivery often borrows principles from those developed for the delivery of plasmid DNA for gene therapy applications. Improvements in the design of new carriers focus mainly on the polymer characteristics, attempting to improve the delivery effectiveness of the vector by modifying various polymer features such as backbone chemistry and side-chain length or, increasingly, by incorporating additional functionalities into the vector[6,7,8,9].

Relatively little is known concerning the effect of ODN properties on the interactions between carriers and ODNs. Clearly, the structure and sequence composition are key features of the ODN and have significant implications on its biological interactions, such as its ability to

*To whom correspondence should be addressed. Phone: 732-445-4109 Fax: 732-445-2581 Email: cmroth@rci.rutgers.edu

hybridize with a target mRNA[10] and its resistance to nuclease digestion. For example, ODNs designed to form stable structures, such as hairpins or loops, exhibit better resistance to nuclease digestion as compared to unstructured ODNs[11]. Furthermore, certain applications call for the use of structured ODNs. For example, molecular beacons, which possess a hairpin structure, are fluorescent hybridization probes that are used for quantitation of complementary targets in samples and have been used for visualization of RNA in cells[12,13]. In addition, circular or dumbbell shaped ODNs are used as decoys for transcription factor binding in an alternative approach to inhibit gene expression at the level of transcription[14,15]. Despite its relevance to these applications, relatively little attention has been paid to understanding the molecular biophysics of ODN interactions with carriers such as polymers, or on relating their biophysical characteristics to the biological activity of the vectors[16].

In this study, we tested the interactions between a cationic polymer, poly-L-lysine, and ODNs of different structures (unstructured vs. hairpin). Four ODNs (two unstructured and two hairpin) sequences complementary to the rabbit beta-globin mRNA were selected on the basis of thermodynamic modeling from a dataset used in our previous work[10,17]. Each ODN was 17 nt in length, which is typical for antisense studies. The structures of the hairpins are shown in Figure 1. For the polymer we chose poly-L-lysine (pLL) as a simple, well-characterized, cationic polymer, due to its ease of availability and handling and its previous use in DNA delivery studies[18-21]. We probed both the association and dissociation behavior of pLL-ODN complexes, and found that ODN structure influences significantly its interactions with pLL.

Materials and Methods

Materials

Four 17-mer phosphodiester ODN sequences were used in the study: two unstructured ODNs and two hairpin structured ODNs. The sequences and free energies of unfolding of the ODNs are provided in Table 1. Oligonucleotides were obtained from Integrated DNA Technologies (Coralville, IA). Stock solutions were prepared by reconstituting the pellet in TE (Tris-EDTA) buffer at pH 8 to a final concentration of 1 mg/mL. Poly-L-lysine (pLL) of varying molecular weights was purchased from Sigma (St. Louis, MO). Stock solutions at a concentration of 1 mg/mL were prepared in water. All stock solutions were diluted further in TE buffer as required to prepare solutions of desired concentrations. OliGreen®, a dye that binds strongly to single-stranded DNA, was obtained from Molecular Probes (Eugene, OR). Heparin sodium salt was obtained from Sigma (Cat# H4784).

Preparation of oligoplexes

Oligoplexes were prepared at desired pLL:ODN charge ratios by mixing equal volumes of pLL (of varying concentrations) and ODNs in TE buffer at pH 8. The samples were vortexed briefly, and the solutions were then incubated at room temperature for 10-15 minutes to ensure complex formation. Experimental evidence (stabilization of fluorescence corresponding to free ODN) confirmed that this time was sufficient for complex formation. The pLL:ODN charge ratios were calculated on a molar basis. The complexes were prepared at a final ODN concentration of 5 μg/mL (approx. 1 μM) unless stated otherwise. This concentration is comparable to what is used in antisense experiments[23].

Detection of free ODN using OliGreen®

Complexes between pLL and ODN were prepared at various charge ratios as described above. One hundred microliters of each complex solution was transferred to a 96 well (black-walled, clear-bottom, non-adsorbing) plate (Corning, NY). One hundred microliters of diluted OliGreen® reagent (1:200 in TE buffer at pH 8) was then added to all samples for free ODN detection. We found no changes in polymer-ODN binding even at higher OliGreen®

concentrations (1:100 dilution- data not shown), which implies that that the OliGreen® concentration did not have an effect on the binding. Fluorescence measurements were made after a 3-5 minute incubation using a Cytofluor (Applied Biosystems, CA), at excitation and emission wavelengths of 485 and 520 nm, respectively, and a voltage gain of 55. All measurements were corrected for background fluorescence from a solution containing TE buffer and diluted OliGreen® reagent.

ODN release studies

Fifty microliters of heparin solution (at various concentrations prepared in TE buffer at pH 8) were added to 50 μL of complex solution (final ODN concentration of 2 μg/mL, ~0.4 μM) in a 96 well (black-walled, clear-bottom, non-adsorbing) plate. One hundred microliters of diluted OliGreen® reagent was added, and the solution was mixed manually using a multichannel pipette. Fluorescence measurements were made immediately using the Cytofluor plate reader. The kinetics of ODN release from the complexes were obtained by recording fluorescence at an interval of 1 minute for up to 30 minutes. Both the kinetics and the heparin dose response of ODN release were recorded for all pLL-ODN complexes at pLL:ODN charge ratios of 2:1 and 5:1. The percentage of ODNs released was calculated from the fluorescence (*F*) values as:

$$\%\ ODN \quad released = \frac{[F\ (complex+heparin) - F\ (ODN+heparin)]}{[F\ (complex) - F\ (ODN+heparin)]} \times 100\% \tag{1}$$

Modeling Polymer-ODN complexation

The complexation of DNA with polymers used for delivery is typically expressed in terms of fraction DNA bound (or not bound) as a function of the charge ratio of total polymer added to DNA. We first attempted to utilize simple stoichiometric models based on charge neutralization to describe the binding curves; however, these did not accurately reproduce the correct shape of the binding curves or their lack of dependence over a large range of polymer molecular weights (not shown). Consequently, we adopted models previously used to study oligomer adsorption for this task.

First, we employed the McGhee-von Hippel isotherm for the binding of ligands that occupy multiple sites to an infinite lattice. This model has been used previously, among other applications, for the interpretation of oligocation/oligonucleotide binding[24]. The McGhee-von Hippel isotherm relates via statistical thermodynamics a quantity, *v*, equal to the moles bound of ligand per mole of lattice sites, to the free ligand concentration [*L*], the number of sites occupied per ligand *n*, and the equilibrium constant *K* for binding of a ligand to a site:

$$\frac{v}{[L]} = K(1 - nv)\left[\frac{1 - nv}{1 - (n-1)v}\right]^{n-1} \tag{2}$$

Putting this into terms of the fraction of oligonucleotide bound, *f*, and the pLL:ODN charge ratio, *r*, results in the implicit expression:

$$\frac{f}{1-f}\frac{1}{nD_T r} = K\left(1 - \frac{f}{r}\right)\left[\frac{1 - f/r}{1 - \left(\frac{n-1}{n}\right)f/r}\right]^{n-1} \tag{3}$$

where D_T is the total concentration of ODN in the system (bound plus free). While this cannot be solved explicitly for either *f* or *r*, it can be solved for *f* in terms of the ratio $\phi = f/r$. The resulting expression was used to generate plots of *f* vs. *r* by enumerating *f* as ϕ is increased from zero towards one, then using the solution for *f* to calculate the corresponding *r* as $r = f/\phi$:

$$f=1-\frac{1}{n\kappa}\frac{\phi}{1-\phi}\left[\frac{1-\left(\frac{n-1}{n}\right)\phi}{1-\phi}\right]^{n-1} \quad (4)$$

where κ is a dimensionless parameter equal to KD_T.

We also utilized an extension to the McGhee-von Hippel isotherm in which the finite size of the receptor (taken here to be pLL) is taken into account. The key feature of this approach, originally developed by Epstein[25] and later applied for analysis of oligocation/oligonucleotide binding[26], is the computation of the number of potential configurations, Ω_j, of j ligands each covering n sites out of a total of N total sites per receptor:

$$\Omega_j=\frac{[N-(n-1)\,j]\,!}{j!\,(N-nj)\,!} \quad (5)$$

This factor is used in the computation of a partition function, Ξ, which is summed over the possible number of ligands bound, ranging from zero to J_{max}, which is the nearest integer less than or equal to N/n:

$$\Xi=\sum_{j=0}^{J_{\max}}(K\,[D_F])^j\Omega_j \quad (6)$$

where $[D_F]$ is the concentration of free (unbound) ODN. The isotherm is then found by summation of the probabilities of all possible receptor occupancies:

$$\nu=\frac{1}{N\Xi}\sum_{j=0}^{J_{\max}}j(K\,[D_F])^j\Omega_j \quad (7)$$

We again wished to express this in terms of fraction ODN bound and pLL:ODN charge ratio, which was accomplished employing the relations $[D_F] = D_T(1\text{-}f)$ and $f = nvr$, to obtain:

$$\frac{Nf}{nr}=\frac{\sum_{j=0}^{J_{\max}}j[\kappa(1-f)]^j\Omega_j}{\sum_{j=0}^{J_{\max}}[\kappa(1-f)]^j\Omega_j} \quad (8)$$

This equation is easily solved explicitly for r in terms of f and was used to compute the charge ratios corresponding to a range of bound ODN fractions.

Results

Our primary goal was to evaluate the association-dissociation behavior of complexes containing pLL and ODNs of differing structures (unstructured and hairpin structured) at varying charge ratios. The length, 17 nucleotides, and concentration, 1 μM, of the ODNs were chosen to be relevant to use in antisense technology and were held constant throughout. The study of polymer-DNA complexes for gene or oligonucleotide delivery requires a reagent to detect the DNA and a means to determine the state of the DNA (bound or free). To avoid issues associated with the use of attached fluorescent dyes, detection of ODN was performed using OliGreen®, a commercially available dye that binds to single-stranded DNA and does not fluoresce significantly in the absence of DNA or in the presence of polymer alone (results not shown). Complex formation between DNA and polymer leads to inaccessibility of the dye to ODN and a resultant decrease in fluorescence intensity with increasing polymer concentration. Thus, the fluorescent signal measurement corresponds to the uncomplexed ODN in solution. This assay procedure is analogous to previous approaches for studying plasmid complex formation with polymers and lipids using DNA-binding dyes[27-29].

First, we assessed pLL-ODN binding as a function of pLL:ODN charge ratio for a single pLL molecular weight. As expected, for all ODNs, the fluorescence signal decreased, indicating that more ODNs were incorporated into complexes, with increasing charge ratios (Figure 2). At lower charge ratios, both unstructured and hairpin ODNs behave more or less similarly. However, at charge ratios of one and above, almost all the hairpins were complexed, while significant quantities of unstructured ODNs remained in solution, indicating less extensive complex formation or ODNs otherwise in a dye-accessible state.

Since pLL-ODN binding was found to depend on ODN structure at a single pLL molecular weight, we tested the effect of varying pLL molecular weight on these interactions. We prepared complexes of each ODN with pLL of five different molecular weights ranging from 500 Da to 574 kDa and determined the amount of free ODN in solution as a function of the polymer:ODN charge ratio. As shown in Figure 3, for each ODN, the pLL-ODN association did not vary significantly with pLL molecular weight except at the lowest molecular weight studied, 500 Da. At this molecular weight, complex formation was extremely inefficient. At all other pLL molecular weights, pLL-ODN association depended on ODN structure. Hairpins exhibited greater association with pLL than unstructured ODNs, particularly at high charge ratios.

In order to understand better the lack of molecular weight dependence on pLL-ODN complexation behavior for most of the pLL range tested, we compared our results with the predictions of various theoretical models. First, several stoichiometric models, including the Scatchard and Hill isotherms as well as a formulation based on charge equivalents, were tested. All these fail to capture the lack of pLL molecular weight dependence over a wide range and in most cases do not follow very well the shape of the observed binding curve. Next, we utilized the McGhee-von Hippel isotherm, which describes the extent of binding of a “large ligand”, i.e., one that covers multiple binding sites, to an infinite lattice (receptor). Since, at all but the lowest pLL molecular weight, the number of pLL charges per molecule greatly exceeds that for the ODN, we took pLL as the receptor and ODN as the ligand. The charge per ODN is fixed at $n = 17$ and the charge per pLL, N, is determined from its molecular weight (Table 2). By expressing this isotherm in terms of the variables used in analysis of polymer-DNA complexes for DNA delivery – fraction DNA complexed (f) and polymer:DNA charge ratio (r) – we obtained Eq. (3), which has no dependence on polymer molecular weight and a single parameter that is not determined from molecular structure, namely the dimensionless affinity κ. Parametric plots of this model show that binding is strongly affected by low values of the affinity, whereas the dependence is much weaker for values of $\kappa > 1$ (Figure 4a). The experimental data for structured ODNs at all pLL molecular weights from 9,800 to 574,000 Daltons falls within the band of $1 < \kappa < 5$, but due to the insensitivity of the data in this region we did not attempt to explicitly fit the value of κ to the data.

Since the lack of polymer molecular weight dependence in the McGhee-von Hippel model is due to treating the polymer as an infinite array, we relaxed this approximation by implementing a finite size formulation of the isotherm[25,26]. Calculation of the number of system configurations was accomplished using Eq. (5), and the isotherms were subsequently determined by application of Eq. (8). The number of configurations rises dramatically with polymer molecular weight and proved problematic under conditions corresponding to the 574,000 MW pLL. Thus, we computed isotherms corresponding to the experimentally tested molecular weights from 9,800 to 84,000, along with a lower molecular weight of 4,000, which provides a polymer charge number of $N \sim 31$, still greater than the ODN charge number of $n = 17$. The results show that the lack of pLL molecular weight dependence is maintained over the range of 9,800 to 84,000 Daltons. As N is lowered to values approaching n (such as in the 4000 Da case shown), a shift of the binding curves to the right is predicted, though the effect

is not nearly as dramatic as observed experimentally when the molecular charge ratio *N*/*n* shifts to values less than 1 (cf. Figure 3).

We studied further the dissociation behavior of these complexes upon exposure to heparin sulfate as a competitive binding agent. Heparin is a negatively charged polysaccharide that has been previously shown to disrupt polymer-ODN complexes. In our study, pLL-ODN complexes were prepared at various conditions, and then heparin was added to dissociate the complexes, releasing ODN into solution. OliGreen® was used to measure the amount of ODN released over 30 minutes. Both the kinetics and heparin dose response of release were recorded. In each measurement, we corrected for changes in background fluorescence due to heparin addition alone. This change was found to be dependent on the heparin concentration (data not shown) and thus was measured and accounted for in each experiment.

The raw data from one such experiment with controls is shown in Figure 5a. For ODN alone, a high and stable fluorescence signal was recorded. The addition of pLL at a 2:1 charge ratio resulted in an almost complete loss of signal, indicative of complex formation. Addition of heparin induced a gradual increase in fluorescence from the baseline, indicating release of the ODN. From the heparin concentration (5 μg/mL = 0.4 μM) and the characteristic time of release (~1 min), we estimate the second-order rate constant for ODN release by heparin to be on the order of 1 μM^{-1} min^{-1}. This value is within the range observed for binding of antisense oligonucleotides to their structured complementary RNA targets[10] and is significantly less than that which would be observed for the diffusion-limited binding of heparin to pLL. Thus, the process is kinetically controlled, and the pLL-ODN complexes are competitively disrupted by addition of heparin.

The kinetics of ODN release from complexes at 2:1 and 5:1 pLL-ODN ratios (at 5 μg/mL heparin concentration) are shown in Figures 5b and 5c, respectively. Consistent with the finding that hairpin ODNs associate to a greater extent with pLL as compared to unstructured ODNs, the pLL-hairpin complexes did not release ODNs very easily. Nearly all of the unstructured ODNs were released out of the complexes within 15-20 minutes, while up to 80% of hairpin ODNs remained bound to pLL at 30 minutes. This effect was relatively insensitive to the two charge ratios used. At both charge ratios, pLL-unstructured ODN complexes dissociated to a greater extent and at a faster rate, releasing more ODNs.

The dose response of ODN release with varying amounts of heparin was determined, using release at the end of 15 minutes as the measurement. As expected, increasing amounts of ODNs were released with higher doses of heparin at a single pLL:ODN charge ratio (Figure 6). At higher polymer:ODN charge ratios, such as 5:1, greater heparin amounts were required to release similar ODN amounts. This is to be expected, since a significant amount of free pLL presumably exists at a charge ratio of 5:1, which the heparin would titrate more easily than complex-bound material. In all cases, nonetheless, unstructured ODNs were released from the complexes at lower heparin doses as compared to hairpins, further underlining the strength of pLL-hairpin interactions.

Discussion

Cellular delivery remains a major hurdle in the utilization of ODN-based applications such as antisense technology[2]. Although vector development for the efficient delivery of ODNs is an active area of research, there are few systematic studies focusing on understanding carrier-ODN interactions for the purpose of rational vector design. Existing studies of the interactions between oligonucleotides and cationic polymers have focused primarily on the salt dependence of binding as a probe of their electrostatic properties[24,26]. Other aspects of these interactions, such as their dependence on molecular structure, kinetics and stability in the presence of other

species, are less well understood. Studies have shown that complexes between pLL and ODNs are multimolecular in composition with several ODNs and multiple pLL chains participating in complex formation[30]. In order to enhance our understanding of these interactions, the ODN structure and pLL molecular weight were varied in this study.

Our assays provided reproducible data probing quantitatively the complexation between the cationic polymer, pLL, and ODNs, which are anionic. For plasmid DNA, electrostatic interactions with cationic polymer lead to condensation of the DNA at a critical ratio of positive to negative charges and the formation of toroidal, rod-shaped or spherical complexes[19]. As a result, complex formation for plasmid DNA is assayed by exclusion of DNA binding dyes such as ethidium bromide. This type of procedure is also employed for polymer-oligonucleotide complexes, even though ODNs do not possess a super-structure to condense in the manner of plasmid DNA. Previous results, as well as those presented here, support the notion that pLL resides on the outside of pLL-ODN complexes since the OliGreen® dye was excluded. The fact that unstructured ODNs exhibited an excess fluorescence even at high charge ratios suggests the possibility that a fraction of the ODN is complexed yet remains accessible to OliGreen®. However, we have also found that unstructured ODNs more effectively displace fluorescently labeled ODNs from pLL-ODN complexes, providing independent confirmation that unstructured ODNs exhibit higher affinity for pLL (results not shown). Moreover, our heparin dissociation studies (Figure 6) also point to a difference in the pLL-ODN interaction with ODN structure.

The dependence of complex formation on ODN structure observed in our work could be due to the differences in charge density distributions of the ODNs. The linear charge density of pLL, which has a charge for roughly each 128 g of molecular weight, is greater than that for an ODN, with a charge for roughly each 330 g of molecular weight. Thus, it is reasonable that decreasing the charge density of pLL or increasing the charge density of ODN would lead to a more symmetric charge distribution and hence to more efficient complexation. Hairpin ODNs provide a higher local concentration of charges as compared to unstructured ODNs, which may allow for a more symmetric interaction with the charge groups in pLL. An effect of DNA charge density on complexation has been found using plasmid DNA of varying topology, where cationic copolymers were shown to bind preferentially to supercoiled DNA compared to linear DNA[31]. Our results suggest that ODN structure may similarly influence the electrostatics of complex formation.

Complex formation is highly inefficient at low pLL molecular weight, which is in agreement with observed trends for polymer-plasmid DNA binding[32]. This molecular weight (500 Daltons by the vendor) is the only one studied for which the amount of charge per pLL molecule is less than that per ODN molecule (Table 2). For higher molecular weights of pLL, there was no difference in pLL-ODN binding with varying pLL molecular weight. These results can be interpreted using isotherms developed for ligands that cover multiple sites upon binding[24, 25]. We applied these isotherms (Eqs. (3) and (8)) assuming that the ODN is the ligand binding to sites on pLL, with sites corresponding to each charge group. Thus, $n = 17$ lattice sites are covered by the ODN upon binding to pLL. For the polymer molecular weights utilized in this study, these isotherms predicted either no (for an infinite lattice) or negligible (for a finite size lattice) dependence on pLL molecular weight. This result is in agreement with the experimental data and is not predicted based on stoichiometric binding between a polycationic polymer molecule and a neutralizing number of oligonucleotides. At the lowest pLL molecular weight, the number of charges per pLL becomes less than that for the ODN. As a result, there is no site on the pLL large enough to accommodate the ODN. The same type of isotherm could then be applied by reversing the roles of ligand and receptor. However, in doing so, it was not possible to obtain a form that was calculable for f and r as in Eq. (8). Nonetheless, we would expect that the interaction would be considerably weaker, as the fundamental adsorption event would

involve four charge groups (for $N = 4$ at pLL MW 500) as opposed to seventeen for all other molecular weights. This large reduction in the affinity of a single adsorption event is likely a major reason for the shift in the binding curve when the number of pLL charges becomes less than the number of ODN charges. Thus, a combination of polymer adsorption isotherms and site number considerations explain the pLL molecular weight dependence of binding. They do not, however, explain the ODN structure effect, as high charge ratios should eventually provide enough binding sites and driving force for ODN adsorption. Since some residual ODN remains accessible to OliGreen®, there are presumably other aggregation or adsorption states being occupied by the ODNs. With a better understanding of what these are, we could incorporate them into the isotherms to produce better agreement with the data.

Polyanion disruption assays, using molecules such as dextran sulfate, poly-L-aspartic acid and heparin, have been used to study the dissociation behavior of carrier-DNA complexes[33]. Here, we used heparin to disrupt the pLL-ODN complexes and found that the release profiles depend on ODN structure. Both the heparin dose response curves and the kinetics of ODN release indicated that the release of the hairpins from the complex was greatly inhibited, presumably due stronger association with pLL. However, the two hairpins, HP1 and HP2, differed in their interactions with pLL. While HP1 release from its complex with pLL, when challenged with heparin, was greatly inhibited, HP2 exhibited intermediate ability to be dissociated from pLL. Examination of the two structures (Figure 1) indicates a difference in the number of bonds as well as the GC content involved in the formation of the hairpin. The ability of the pLL-ODN complex to resist dissociation by heparin addition is likely to depend on both the strength (affinity) of the pLL-ODN interaction as well as its flexibility (entropy). We speculate that the HP1 structure may possess the best combination of affinity enhancement, from the greater charge density in the hairpin structure, and flexibility, from maintaining a sufficient number of single-stranded nucleotides. This combination would foster retention of binding with pLL under heparin challenge.

Heparin, which was used to disrupt the complexes in our studies, is a negatively charged polysaccharide, belonging to a family of glycosaminoglycans (GAGs) that are often enriched in the extracellular matrix. GAGs have been shown to inhibit DNA delivery[34-36]. In our studies, the concentrations of heparin required to induce dissociation and the time scale (minutes) of the dissociation process were of a magnitude to be potentially relevant for cellular delivery of ODNs to living cells. Thus, it may prove useful to employ hairpin structured ODNs to avoid GAG-induced disruption of complexes and to promote other mechanisms of intracellular ODN release.

In summary, we have shown that ODN structure influences the interactions between cationic polymers such as pLL, and ODNs. The structure of ODNs is an important parameter that also influences additional properties relevant for antisense activity, such as its interaction with the mRNA target and the rate of ODN degradation by nucleases. Selection of effective antisense sequences and their efficient cellular delivery are key factors that determine the outcome of an antisense experiment. The fact that ODN structure affects its association with carriers that are used for delivery therefore highlights the importance of ODN properties on vector design and provides another consideration for the rational design and control of carrier mediated ODN delivery.

Acknowledgments

We are grateful for financial support from the Whitaker Foundation (TF 02-002), NIH (R01 GM65913) and a Rutgers Undergraduate Research Fellowship (to S.V.). We also thank Dr. Li Kim Lee and Neha Shah for technical assistance and useful discussions and Prof. Prabhas Moghe for access to the Cytofluor.

References

1. Lee LK, Roth CM. Curr Opin Biotechnol 2003;14:505–511. [PubMed: 14580580]
2. Roth CM, Sundaram S. Annu Rev Biomed Eng 2004;6:397–426. [PubMed: 15255775]
3. Chirila TV, Rakoczy PE, Garrett KL, Lou X, Constable IJ. Biomaterials 2002;23:321–342. [PubMed: 11761152]
4. De Smedt SC, Demeester J, Hennink WE. Pharm Res 2000;17:113–126. [PubMed: 10751024]
5. Hope MJ, Mui B, Ansell S, Ahkong QF. Mol Membr Biol 1998;15:1–14. [PubMed: 9595549]
6. Deshpande MC, Garnett MC, Vamvakaki M, Bailey L, Armes SP, Stolnik S. J. Control. Release 2002;81:185–199. [PubMed: 11992691]
7. Jones NA, Hill IR, Stolnik S, Bignotti F, Davis SS, Garnett MC. Biochim Biophys Acta 2000;1517:1–18. [PubMed: 11118611]
8. Mannisto M, Vanderkerken S, Toncheva V, Elomaa M, Ruponen M, Schacht E, Urtti A. J. Control. Release 2002;83:169–182. [PubMed: 12220848]
9. Tang MX, Szoka FC. Gene Ther 1997;4:823–832. [PubMed: 9338011]
10. Walton SP, Stephanopoulos GN, Yarmush ML, Roth CM. Biophys J 2002;82:366–377. [PubMed: 11751323]
11. Maksimenko AV, Gottikh MB, Helin V, Shabarova ZA, Malvy C. Nucleosides Nucleotides 1999;18:2071–2091. [PubMed: 10549152]
12. Tan W, Wang K, Drake TJ. Curr Opin Chem Biol 2004;8:547–553. [PubMed: 15450499]
13. Bratu DP, Cha BJ, Mhlanga MM, Kramer FR, Tyagi S. Proc Natl Acad Sci U S A 2003;100:13308–13313. [PubMed: 14583593]
14. Aguilar L, Hemar A, Dautry-Varsat A, Blumenfeld M. Antisense Nucleic Acid Drug Dev 1996;6:157–163. [PubMed: 8915499]
15. Lee IK, Ahn JD, Kim HS, Park JY, Lee KU. Curr Drug Targets 2003;4:619–623. [PubMed: 14577652]
16. Meidan VM, Glezer J, Amariglio N, Cohen JS, Barenholz Y. Biochim. Biophys. Acta-Gen. Subj 2001;1568:177–182.
17. Walton SP, Stephanopoulos GN, Yarmush ML, Roth CM. Biotechnol Bioeng 1999;65:1–9. [PubMed: 10440665]
18. Forrest ML, Pack DW. Mol Ther 2002;6:57–66. [PubMed: 12095304]
19. Liu G, Molas M, Grossmann GA, Pasumarthy M, Perales JC, Cooper MJ, Hanson RW. J. Biol. Chem 2001;276:34379–34387. [PubMed: 11438546]
20. Molas M, Bartrons R, Perales JC. Biochim. Biophys. Acta-Gen. Subj 2002;1572:37–44.
21. Wagner E, Ogris M, Zauner W. Adv Drug Deliv Rev 1998;30:97–113. [PubMed: 10837605]
22. Mathews DH, Disney MD, Childs JL, Schroeder SJ, Zuker M, Turner DH. Proc Natl Acad Sci U S A 2004;101:7287–7292. [PubMed: 15123812]
23. Jayaraman A, Walton SP, Yarmush ML, Roth CM. Biochim Biophys Acta 2001;1520:105–114. [PubMed: 11513951]
24. Zhang W, Bond JP, Anderson CF, Lohman TM, Record MT Jr. Proc Natl Acad Sci U S A 1996;93:2511–2516. [PubMed: 8637905]
25. Epstein IR. Biophys Chem 1978;8:327–339. [PubMed: 728537]
26. Zhang W, Ni H, Capp MW, Anderson CF, Lohman TM, Record MT. Biophys J 1999;76:1008–1017. [PubMed: 9916032]
27. Wiethoff CM, Gill ML, Koe GS, Koe JG, Middaugh CR. J Pharm Sci 2003;92:1272–1285. [PubMed: 12761816]
28. Tsai JT, Furstoss KJ, Michnick T, Sloane DL, Paul RW. Biotechnol Appl Biochem 2002;36:13–20. [PubMed: 12149118]
29. Choi SJ, Szoka FC. Anal. Biochem 2000;281:95–97. [PubMed: 10847615]
30. Lucas B, Van Rompaey E, De Smedt SC, Demeester J, Van Oostveldt P. Macromolecules 2002;35:8152–8160.
31. Bronich TK, Nguyen HK, Eisenberg A, Kabanov AV. J. Am. Chem. Soc 2000;122:8339–8343.
32. Godbey WT, Wu KK, Mikos AG. J Biomed Mater Res 1999;45:268–275. [PubMed: 10397985]

33. Zelphati O, Szoka FC. Proc. Natl. Acad. Sci. U. S. A 1996;93:11493–11498. [PubMed: 8876163]
34. Hawley P, Gibson I. Antisense Nucleic Acid Drug Dev 1996;6:185–195. [PubMed: 8915503]
35. Mislick KA, Baldeschwieler JD. Proc Natl Acad Sci U S A 1996;93:12349–12354. [PubMed: 8901584]
36. Ruponen M, Ronkko S, Honkakoski P, Pelkonen J, Tammi M, Urtti A. J. Biol. Chem 2001;276:33875–33880. [PubMed: 11390375]

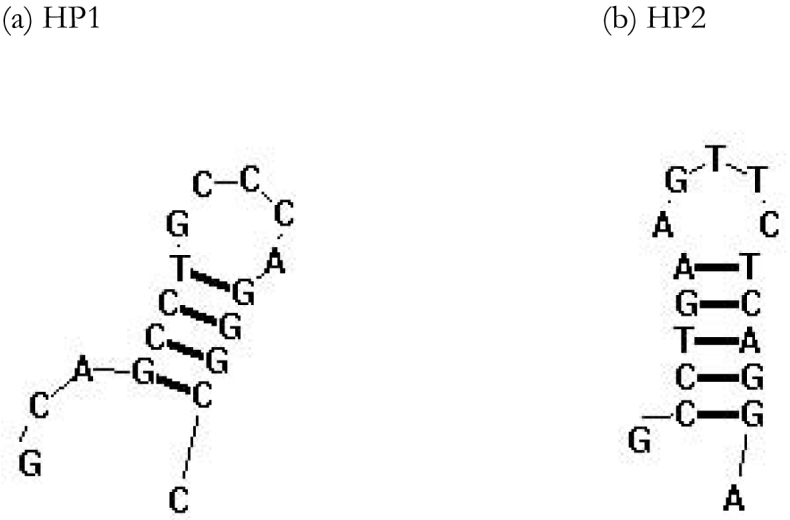

Figure 1.
Structures of hairpin ODNs (a) HP1 and (b) HP2 (Generated using RNAStructure 4.1 software) 22

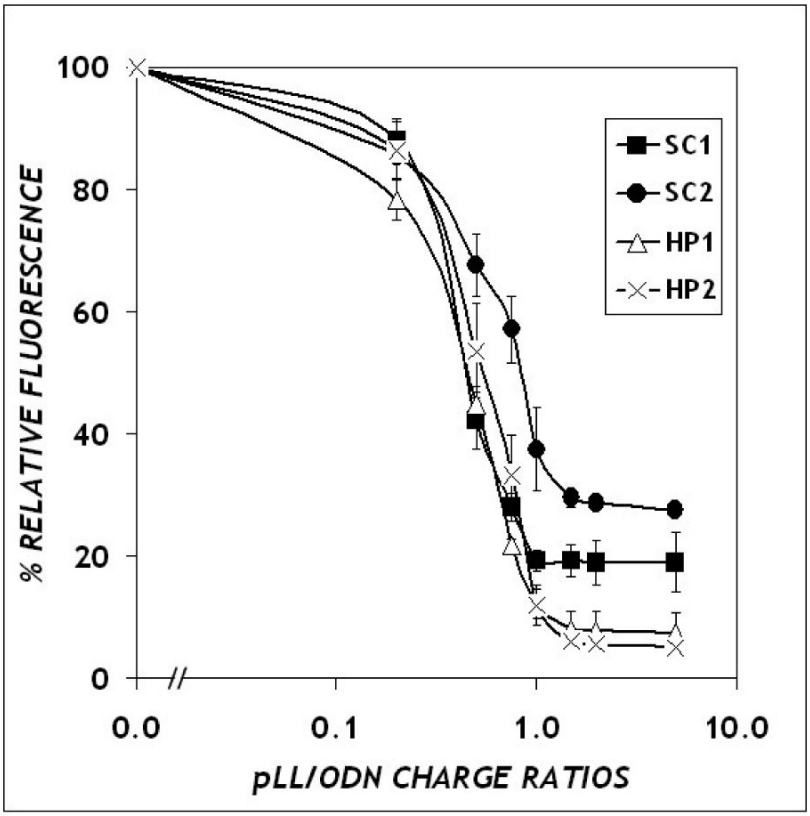

Figure 2.

Effect of ODN structure on complex formation. The OliGreen® fluorescence was measured after forming complexes between ODN (in an amount corresponding to a final concentration of 1 μM) and the amount of pLL necessary to attain the indicated charge ratios. Filled symbols represent the unstructured ODNs, and open symbols (or X) represent hairpin structured ODNs. Data represent the mean ± standard deviation of at least 3 replicates.

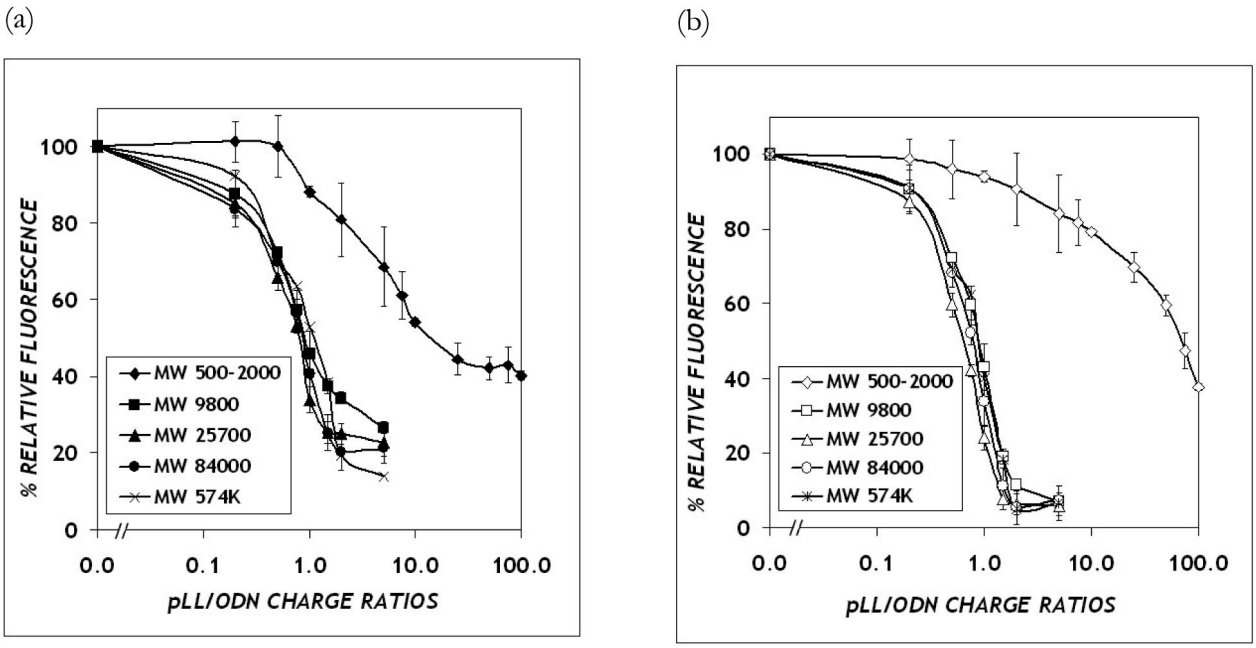

Figure 3.
Effect of pLL molecular weight on complex formation (determined using the OliGreen® assay) for individual ODNs of various structures: (a) Unstructured ODNs, (b) Hairpin ODNs. Data represent the mean ± standard deviation of at least 3 replicates.

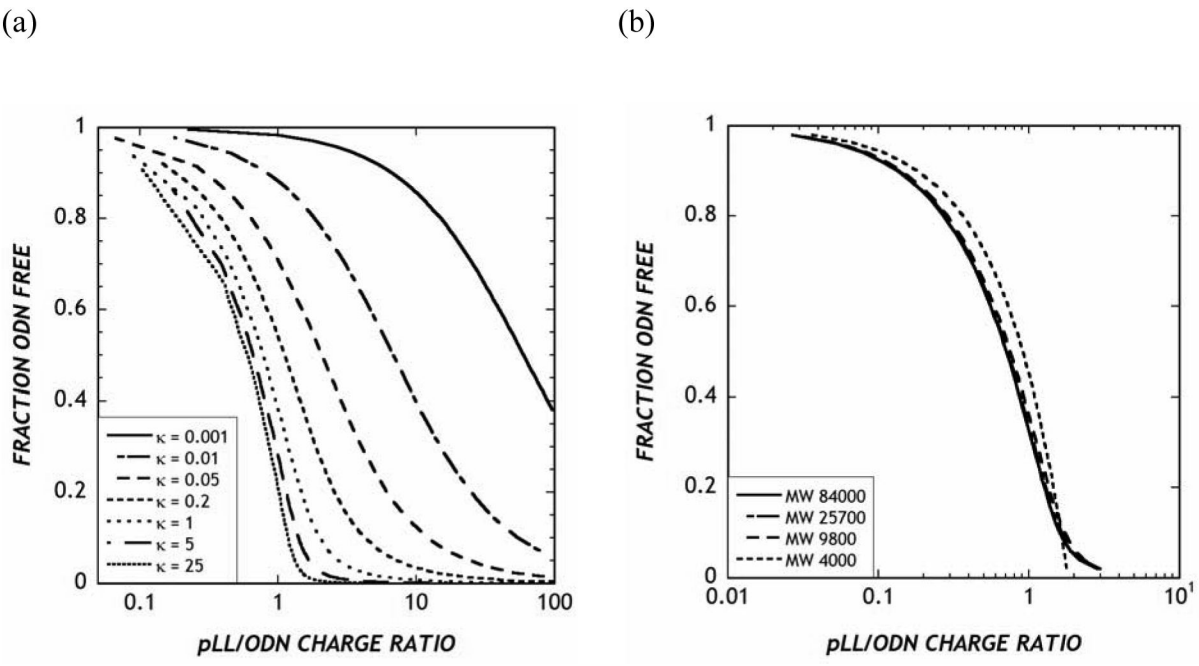

Figure 4.

Model predictions of pLL-ODN complexation behavior. (a) Predictions of the McGhee-von Hippel isotherm at varying values of dimensionless affinity, κ; (b) Polymer molecular weight dependence, calculated using the finite size correction to the McGhee-von Hippel isotherm[25,26].

(a)

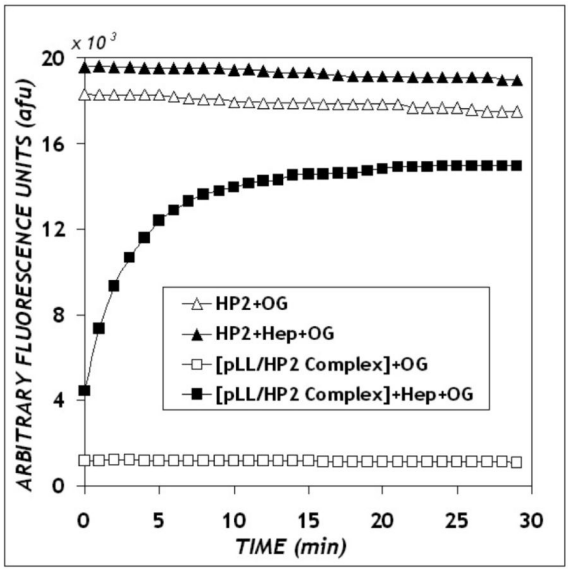

(b)

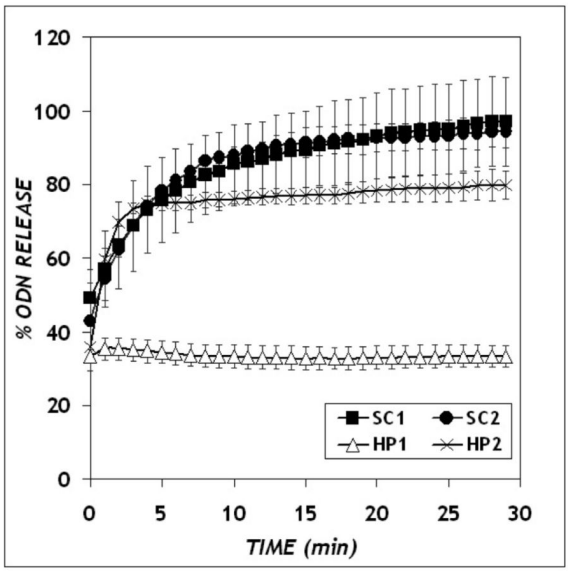

(c)

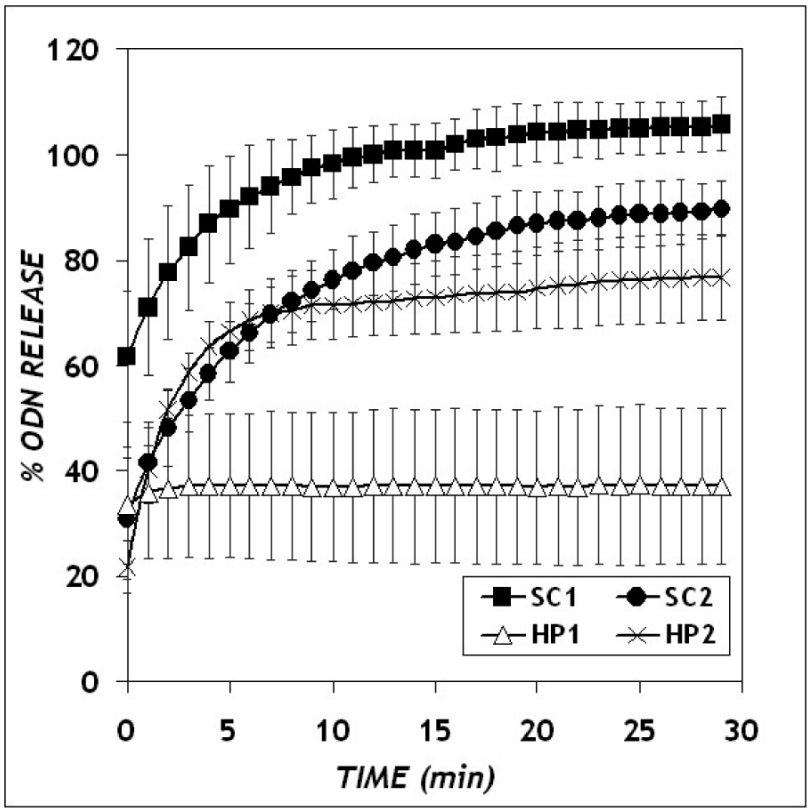

Figure 5.
ODN release kinetics from pLL-ODN complexes: (a) Raw data (b) Charge ratio 2:1, heparin concentration 5 μg/mL (c) Charge ratio 5:1, heparin concentration 10 μg/mL. Data represent the mean ± standard deviation of at least 3 replicates.

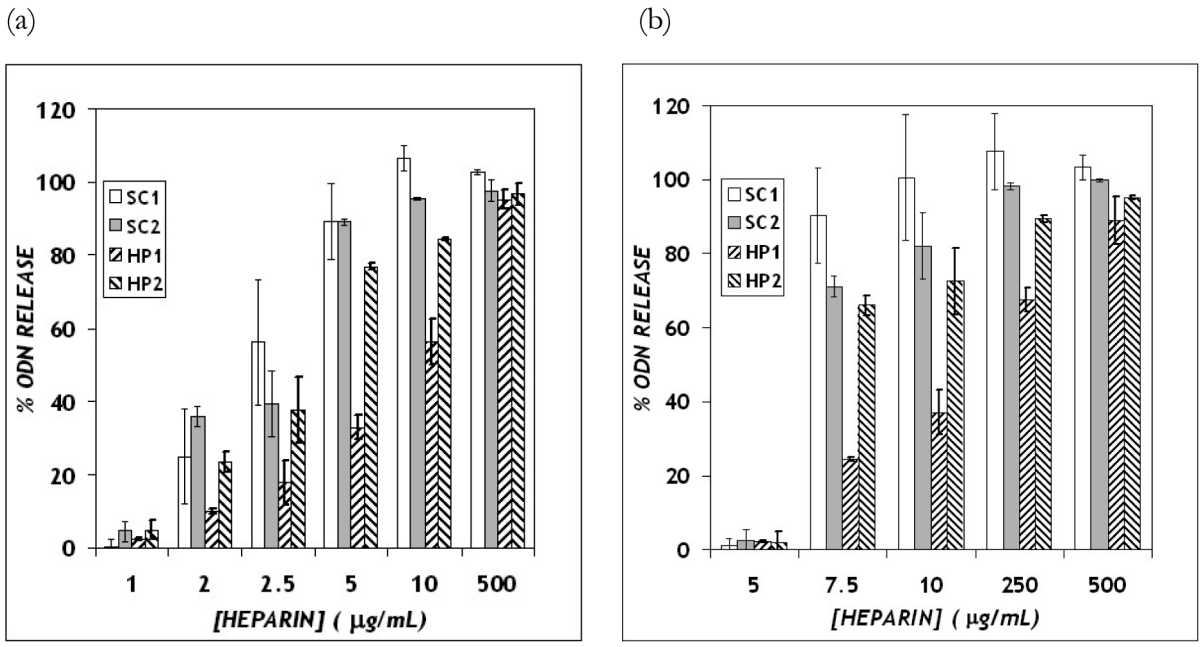

Figure 6.

Heparin dose response curves of the release of unstructured (shaded bars) and hairpin structured (hatched bars) ODNs from pLL-ODN complexes. (a) Charge ratio 2:1, (b) Charge ratio 5:1. Data represent the mean ± standard deviation of at least 3 replicates.

Table 1

Free energy of unfolding of hairpin-structured and unstructured ODNs

ODN name	ODN sequence	ΔG unfolding (kcal/mol)
SC1	5'-ATT-GCA-AGT-AAA-CAC-AG-3'	0
SC2	5'-AGC-TTG-TCA-CAG-TGC-AG-3'	0
HP1	5'-GCA-GCC-TGC-CCA-GGG-CC-3'	2.1
HP2	5'-GCC-TGA-AGT-TCT-CAG-GA-3'	3.9

Table 2

Ratio of molecular charges of pLL to ODN

M_{pLL} (Da)	N	N/n
500	4.0	0.24
9,800	77	4.5
25,700	200	12
84,000	660	38
574,000	4,500	270